DOE/NASA/5266-1
NASA CR-182215

[redacted]

P-20

Comparison of NASA Lewis Research Center's Performance Code's Pressure-Drop Model Predictions to Stirling Engine Working-Space Flow Test Data

Timothy J. Sullivan
Sverdrup Technology, Inc.
NASA Lewis Research Center Group

December 1988

Date for general release December 1990

Prepared for
NATIONAL AERONAUTICS AND SPACE ADMINISTRATION
Lewis Research Center
Under Contract NAS3-25266

for
U.S. DEPARTMENT OF ENERGY
Conservation and Renewable Energy
Office of Vehicle and Engine R&D

DISCLAIMER

Printed in the United States of America

Available from
National Technical Information Service
U.S. Department of Commerce
5285 Port Royal Road
Springfield, VA 22161

NTIS price codes[1]
Printed copy:
Microfiche copy: A01

[1]Codes are used for pricing all publications. The code is determined by the number of pages in the publication. Information pertaining to the pricing codes can be found in the current issues of the following publications, which are generally available in most libraries: *Energy Research Abstracts (ERA); Government Reports Announcements* and Index (*GRA* and I); *Scientific and Technical Abstract Reports (STAR);* and publication, NTIS-PR-360 available from NTIS at the above address.

DOE/NASA/5266-1
NASA CR-182215

Comparison of NASA Lewis Research Center's Performance Code's Pressure-Drop Model Predictions to Stirling Engine Working-Space Flow Test Data

Timothy J. Sullivan
Sverdrup Technology, Inc.
NASA Lewis Research Center Group
Cleveland, Ohio 44135

December 1988

Prepared for
National Aeronautics and Space Administration
Lewis Research Center
Cleveland, Ohio 44135
Under Contract NAS3-25266

for
U.S. DEPARTMENT OF ENERGY
Conservation and Renewable Energy
Office of Vehicle and Engine R&D
Washington, D.C. 20545
Under Interagency Agreement DE-AI01-85CE50112

COMPARISON OF NASA LEWIS RESEARCH CENTER'S PERFORMANCE CODE'S PRESSURE-DROP MODEL PREDICTIONS TO STIRLING ENGINE WORKING-SPACE FLOW TEST DATA

Timothy J. Sullivan
Sverdrup Technology, Inc.
NASA Lewis Research Center Group
Cleveland, Ohio 44135

E-4444

SUMMARY

In support of the U.S. Department of Energy's Stirling Engine Highway Vehicle Systems program, NASA Lewis Research Center's Stirling engine performance code's pressure-drop model was validated in this study for steady flow conditions; the purpose for validating the pressure-drop computer model was to aid in improving the accuracy of the overall Stirling engine performance predictions. The validation was accomplished by comparing P-40 Stirling engine working-space pressure-drop predictions to experimental data, for various steady state flow test conditions. This report includes details of the flow testing results as well as the working-space pressure-drop predictions.

After initial comparisons were made between predictions and flow test data, improvements to the P-40 working-space pressure-drop model were made. The changes included accounting for flow friction in the engine component connecting ducts and increasing the detail in predicting pressure variation due to cross sectional area changes. After these improvements were included, the working space pressure-drop predictions and the flow rig data agreed within the error bands of the test data and the predictions.

This study was conducted for steady flow conditions, because steady state pressure-drop correlations are used in the NASA Stirling engine performance code. In order to complete the pressure-drop model evaluation, the effect of oscillating flow on Stirling engine pressure drop needs to be further investigated.

INTRODUCTION

This study was a step in validating NASA Lewis Research Center's Stirling engine performance code's pressure-drop model. This work was accomplished by comparing P-40 Stirling engine working-space pressure-drop predictions to experimental data, for various steady flow test conditions. The P-40 is a double acting, four-cylinder Stirling engine capable of producing approximately 40 kW of brake power (ref. 1). The P-40 working space includes: the expansion-space, heater tubes, regenerators (2 per cycle), coolers (2 per cycle), compression space, and connecting ducts; the P-40 Stirling engine working space is shown schematically in figure 1.

The calculation of engine component pressure drop is crucial for accurately predicting overall performance. The NASA Lewis, nodal analysis, Stirling engine performance code (ref. 2) uses steady state correlations to calculate engine component pressure drops during each small numerical time

step; it therefore approximates the unsteady or oscillating flow pressure drops. If this approximation to oscillating flow is accurate, then comparing steady flow pressure-drop predictions to actual steady flow data serves as an accurate evaluation of the Stirling engine performance code's pressure-drop model. The effects of oscillating-flow are currently being investigated by Seume and Simon (ref. 3), Wood et al. (ref. 4), and A. Dybbs (private communication from A. Dybbs, Case Western Reserve University, Cleveland Ohio).

In the past Stirling engine individual component pressure-drop predictions were evaluated by comparing them to experimental flow test data. This flow rig has been used for Stirling engine component pressure-drop testing (documented in ref. 5 by Allen and Cairelli); the present pressure-drop computer model contains a correlation for the P-40 regenerator friction factor which was obtained from Allen's data and is included in appendix A. The objective of this study is to evaluate the entire working-space pressure-drop model, which also includes pressure drops that are caused by component transitions.

This validation of the P-40 Stirling engine steady flow pressure-drop model was accomplished by first collecting flow test data for the P-40 working space. These flow test data represented a range of operating conditions similar to that of the P-40 Stirling engine. This report gives details of the flow rig test section, the operation of the flow rig, the flow test conditions, and the pressure-drop computer model. Next, predictions were made for the same steady flow conditions using the working-space pressure-drop computer model. Finally, comparisons between actual and predicted pressure drops were made, resulting in improvements to the working-space pressure-drop model.

This work was done in support of the U.S. Department of Energy (DOE) Stirling Engine Highway Vehicle Systems program. NASA Lewis Research Center, through interagency agreement DE-AI01-85CE50112 with DOE, is responsible for management of the project under the program direction of the DOE Office of Transportation Systems, Heat Engine Propulsion Division.

APPARATUS AND PROCEDURE

Flow Rig Description

A schematic of the flow rig is shown in figure 2. This flow rig is used to measure test section static pressure difference dP for various inlet gas pressures and mass flow rates. The gas used in this flow rig is pure nitrogen at a test section temperature of approximately 0 °C. The gas pressure is limited to 10.3 MPa (1500 psi) gage by the relief valve. In figure 2, valve A is used to adjust the flow meter gas pressure. Valve B is used to adjust the mass flow rate, and valve C is used to adjust the test section gas pressure. The flow meter pressure of 6.8 MPa was chosen to allow for both linear performance of the flow meter pressure-difference dP transducer (pressure-transducer voltage relationship) and sonic flow at valve B, for all flow conditions. Sonic flow results in a variation in the test section pressure not significantly affecting the mass flow rate.

The flow meter and test section transducers feed data into the central data recording system (ESCORT) (described in ref. 1), which converts the transducers electrical output to pressures and temperatures and calculates the

nitrogen mass flow rate from transducers 1, 2, and 3. Table I describes the instrumentation.

Test Section Description

The test section consisted of one modified P-40 Stirling engine working space. A schematic of the P-40 Stirling engine working space (ref. 1) is shown in figure 1; engine components are pictured in figures 3(a) and (b). The pistons and seal housings were replaced with two "cylinder vents" and one "cylinder plug" in order to achieve approximately the same cylinder flow distribution as that set up by the piston motion in the Stirling engine. A flow testing insert was fabricated to provide a high pressure seal between the top "cylinder vent" and the engine block. A schematic of the assembled test section is shown in figure 4.

Operating Conditions

Flow testing dimensionless parameters matched those for the P-40 Stirling engine, which uses hydrogen (H_2) gas. Fluid flow matching, at design conditions, was given in terms of Reynolds number Re and Mach number M. The flow testing boundary conditions were as follows: the gas was nitrogen (N_2), the gas temperature was 0 °C, and the pressure was limited to 10.3 MPa (1500 psi).

Matching design conditions in terms of Re. - The N_2 absolute viscosity, at a relatively low temperature, was approximately equal (error = 1.3 percent) to the Stirling engine's spacial and time averaged H_2 absolute viscosity at a relatively high temperature. Thus, the values of Re matched when working-space mass flow rates matched. As predicted from the NASA Lewis Stirling engine performance code, the mass flow rate at design conditions was 113.4 g/s.

Matching design conditions in terms of M. - The maximum value of M predicted by the NASA Lewis Stirling engine performance code was 0.15 in the cooler/compression-space connecting ducts. Knowing the appropriate N_2 sonic velocity and using an expression for the gas mass flow rate enabled the test section gage pressure to be calculated as 2.2 MPa. At a location other than the cooler/compression-space connecting ducts, the flow testing M is higher than its counterpart in the P-40 Stirling engine (but is still less than the maximum M of 0.15); this is due to relatively isothermal conditions within the test section. Because of the low values of M, in both the P-40 Stirling engine and the test section, the flow can be considered incompressible and differences between the values of M become insignificant. Therefore, the flow testing M is considered matched to M within the P-40 Stirling engine at design conditions.

Approximation to off-design operating conditions. To match the off-design range of P-40 Stirling engine mean gas pressures, the test section gas pressure was varied from maximum (2.2 MPa) to one-third of maximum. To match the off-design P-40 Stirling engine speed range, the N_2 mass flow rate was varied from maximum (113.4 g/s) to one-third maximum; also the mass flow rates varied proportionally to gas pressure variations. Table II shows the flow testing operating conditions. By reversing the orientation of the test section, testing with mass flow in either direction could be accomplished.

Procedure for Collecting Experimental Data

The procedure for conducting a pressure-drop flow test is described below; refer to figure 2 for valve locations. The instrumentation was first calibrated prior to flow testing. Valve A (pressure regulator) was adjusted to obtain a flow meter pressure of 6.8 MPa. Valve B was adjusted to obtain the desired mass flow rate. Valve C was adjusted to obtain the desired test section inlet pressure. Adjustment of valves B and C is continued until the test section flow reaches the desired steady state conditions. After the flow perturbations settle out, the displayed data from ESCORT, the central data recording system, is printed.

Pressure-Drop Simulation

The NASA Lewis Stirling engine performance code's pressure-drop model (ref. 2) was modified to predict only steady flow pressure drop for the flow testing conditions and is referred to as the "pressure-drop simulation." The inputs to the pressure-drop simulation were: gas gage-pressure P and gas temperature T in the test section, N_2 mass flow rate, and the barometric pressure on the particular day of testing.

The steps for simulating the test section pressure drop are given below in outline form. Friction factor correlations are included in appendix A. $F(x,y)$ means F is a function of variables x and y.

(1) Input operating conditions.

(2) Calculate gas density (P,T) for N_2, by using a "real gas" relationship.

(3) Calculate gas viscosity (T) for N_2, at $P = 1.5$ MPa (average gas pressure).

(4) Calculate dP_1 (area change: expansion-space/heater tubes).

(5) Calculate dP_2 (elbows: heater tubes).

(6) Calculate dP_3 (friction: heater tubes, regenerators (2), coolers (2)).

(7) Calculate dP_4 (area change: heater tubes/regenerators).

(8) Calculate dP_5 (area change: regenerators/coolers).

(9) Calculate dP_6 (area change: coolers/compression-space).

(10) Calculate dP_7 (elbow: cooler/compression-space connecting ducts).

(11) Calculate dP_t = summation of dP_i $(i = 1 \text{ to } 7)$.

(12) Print: input conditions, dP_t, and dP_i $(i = 1 \text{ to } 7)$.

The following assumptions were used in the simulation:

(1) Flow thermodynamic and transport "real" properties are constant for each simulation.

(2) Flow is steady, one-dimensional, "incompressible", and adiabatic; thus gas pressure drop depends only on kinetic energy and thermal energy changes. Calculations showed that heat transfer to the N_2 gas during flow testing was negligible.

(3) Friction factors and "minor" loss coefficients depend only on Re and component geometry.

(4) dP_i (area changes) calculations assume fully developed flow prior to the area changes.

Pressure-Drop Simulation Improvements

After comparisons were made between baseline pressure-drop predictions and actual flow test data, improvements were made to the pressure-drop simulation. A heater-tube manifold flow friction correlation was added to the model. Figure 1 shows locations of both heater-tube manifolds, relative to other components in the working space. The assumption was made that the heater-tube manifold pressure drop was that for a simple tube shape using an average manifold hydraulic diameter, average flow path length, and an exit mass flow rate; this simplified pressure-drop model agreed well with a complex pressure-drop model which included the effects of cross-sectional area change and mass flow rate variation in the streamwise direction. Figure 5 shows a simplified sectional view of a heater-tube manifold, which is characteristic of both heater-tube manifolds. The correlation for the heater-tube manifold friction factor is included in appendix A.

A correlation for cooler/compression-space connecting duct flow friction was also added to the pressure-drop simulation and is included in appendix A.

The effect of area changes between the coolers and compression space was revised to now include: cooler tubes/cooler-tube manifold area change, cooler-tube manifold/connecting duct area change, and connecting ducts/compression space area change.

Table III shows P-40 Stirling engine dimensions used for the above revisions to the working-space pressure-drop model. Dimensions for the heater-tube manifolds and the cooler/compression-space connecting ducts are approximate because of complexities of the real engine geometry.

RESULTS AND DISCUSSION

Baseline Pressure-Drop Comparison

For the range of flow testing conditions, the steady flow, P-40 Stirling engine working-space pressure drop was underpredicted by an average of 5.2 percent. Figure 6(a) shows predictions and test data for mass flow from the expansion space to the compression space; likewise, figure 6(b) shows data for mass flow from the compression space to the expansion space. In general,

the percentage error in predicting pressure drop remained relatively constant for increasing mass flow rate and for both flow directions.

Improved Pressure-Drop Comparison

After making the improvements to the P-40 working-space pressure-drop model (described in the APPARATUS AND PROCEDURE section), the absolute error in the predicted pressure drop decreased from 5.2 to 2.3 percent. The results are shown in figures 6(a) and (b).

At the maximum N_2 mass flow rate and maximum gas pressure and with flow direction from the expansion space to the compression space, the discrepancy in the baseline predicted pressure drop was -9.0 kPa. After improving the pressure-drop model, 50 percent of that discrepancy was accounted for by modeling flow friction for the heater-tube manifolds and the coolers/compression-space connecting ducts. Increased accuracy in modeling pressure drop due to the coolers/compression-space area changes accounted for an additional 34 percent of the baseline discrepancy.

Notice that the curvatures of experimental and predicted pressure-drop curves are slightly different. Theoretically this is due to slight errors in thermodynamic or transport properties, errors in pressure-drop correlations, or unaccounted for pressure drop.

Flow Rig Error Analysis

Uncertainty existed in the measurement of: test section and flow meter (venturi type) gas temperature, gas pressure, and gas pressure difference, venturi throat diameter, and P-40 Stirling engine dimensions. Estimated error bands for the flow rig instrumentation are shown in table I. Because some of the above parameters are input into the pressure-drop simulation, uncertainty is introduced into the prediction of working-space pressure drop also.

The uncertainty in experimental data was a result of mass flow rate and test section pressure difference uncertainty and appears as a "square" on figure 7. The curves show predicted pressure-drop uncertainty; error analysis data derived for higher pressures were not included in this report but are similar to figure 7. Details concerning the flow rig error analysis calculations are included in appendix B. Notice there appears to be no error between experimental and predicted pressure drop; this is also the case for data at higher pressures.

CONCLUDING REMARKS

The NASA Lewis pressure-drop computer model was evaluated for the P-40 Stirling engine by comparing working-space pressure-drop predictions to actual P-40 working-space flow test data, under steady flow conditions. After improvements to the pressure-drop model, the results of this study indicated that the pressure-drop model agrees well with the steady flow test data, for a representative range of operating conditions. Furthermore, it is felt that the level of complexity in this working-space pressure-drop model is adequate

for other Stirling engine pressure-drop model because of similar pressure loss mechanisms.

This study was conducted for steady-state conditions, because of the nature of the computer model, the gas flow in a Stirling engine is unsteady or oscillating. In order to complete the working-space pressure-drop evaluation, the effect of this oscillating flow needs to be investigated and is currently underway (described in refs. 3 and 4).

APPENDIX A - FRICTION FACTOR CORRELATIONS

P-40 Regenerator Friction Factor Correlation

If $Re_D < 40.0$ then $f = 91.2829/Re_D^{0.7441}$

If $Re_D > 40.0$ then $f = 33.9152/Re_D^{0.4699}$

where Re_D is the Reynolds number based on the hydraulic diameter and f is the friction factor (not friction coefficient C_f where $C_f = f/4$). Correlation from Allen and Cairelli (ref. 5).

"Smooth Tube" Friction Factor Correlation

The "smooth tube" correlation is used for heater-tube manifolds, cooler/compression-space connecting ducts, and heater and cooler heat exchangers.

If $Re_D < 1500.0$ then $f = 64./Re_D$

If $Re_D > 1500.0$ then $f = 0.1840/Re_D^{0.2}$

Correlation from Kays and London, (ref.6).

APPENDIX B - FLOW RIG ERROR ANALYSIS

An error analysis was performed using the "root-sum square" error equation. The form of this equation used to calculate uncertainty in measured mass flow rate is

$$\pm G = \left[\left(\pm A_t \frac{\partial G}{\partial A_t}\right)^2 + \left(\pm P \frac{\partial G}{\partial P}\right)^2 + \left(\pm T \frac{\partial G}{\partial T}\right)^2 + \left(\pm dP \frac{\partial G}{\partial dP}\right)^2\right]^{1/2}$$

where G is the mass flow rate, A_t is the area of venturi throat, P is the gas pressure, T is the gas temperature, dP is the pressure difference.

The mass flow rate statistical bound (±mass flow rate) was calculated using statistical bounds found in table I and a venturi diameter measurement tolerance of ±0.00005 in. (±0.00125 mm). An appropriate venturi mass flow rate mathematical expression was used to evaluate the partial differentials, dG/d( ). The statistical bound was found to be ±0.284 g/s, evaluated at the maximum mass flow rate and gas pressure. The assumption was made that this statistical bound is correct for all flow conditions.

The uncertainty in the predicted pressure drop was caused by measurement errors in the test section gas temperature and gas pressure, mass flow rate, and engine dimensions. The "root-sum square" error equation was used to calculate the predicted pressure-drop statistical bounds. The "improved" pressure-drop simulation was used to approximate the partial differentials for all flow conditions. This approximation consisted of making two pressure drop predictions, one at standard conditions and one with the independent parameter incremented slightly; the partial differential was then approximated by dividing the difference in predicted pressure drops by the difference in the independent parameters. When evaluating the "engine dimensions" term, the tolerance on all engine dimensions was assumed to be ±0.001 in. (±0.025 mm). The pressure-drop uncertainty was largest when increasing engine component lengths and decreasing component diameters simultaneously.

Predicted pressure-drop uncertainty was mainly due to mass flow rate and test section gas pressure measurement uncertainty; the error in measuring engine dimensions accounted for approximately 23 percent of the total pressure-drop uncertainty.

REFERENCES

1. Kelm, G.G.; Cairelli, J.E.; and Walter, R.J.: Test Results and Facility Description for a 40-Kilowatt Stirling Engine. DOE/NASA/51040-27, NASA TM-82620, 1981.

2. Tew, R.C., Jr.: Computer Program for Stirling Engine Performance Calculations. DOE/NASA/51040-42, NASA TM-82960, 1983.

3. Seume, J.R.; and Simon, T.W.: Effect of Transition on Oscillating Flow Loss in Stirling Engine Coolers and Heaters. Paper presented at the 23rd Intersociety Energy Conversion Engineering Conference, 1988.

4. Wood, G., et al.: Description of Oscillating Flow Pressure-Drop Test Rig. Paper presented at the 23rd Intersociety Energy Conversion Engineering Conference, 1988.

5. Allen, D.; and Cairelli, J.: Test Results of a 40-kW Stirling Engine and Comparison with the NASA Lewis Computer Code Predictions. Proceedings of the 20th Intersociety Energy Conversion Engineering Conference, (IECEC), Vol. 3, Society of Automotive Engineers, 1985, pp. 3.238-3.243 (NASA TM-87050).

6. Kays, W.M.; and London, A.L.: Compact Heat Exchangers. 3rd ed., McGraw-Hill, 1984.

TABLE I. - FLOW TEST RIG INSTRUMENTATION

Label[a]	Parameter	Instrument	Full scale	Error bands
1	Flow meter temperature	Thermocouple	----------	±1 °C
2	Flow meter pressure	Strain gage transducer	10.3 MPa (1500 psi)	±20.6 kPa (±3 psi)
3	Flow meter pressure difference	Strain gage transducer	689.7 kPa (100 psi)	±1.4 kPa (±0.2 psi)
4	Test section temperature	Thermocouple	----------	±1 °C
5	Test section pressure	Strain gage transducer	10.3 MPa (1500 psi)	±20.6 kPa (±3 psi)
6	Test section pressure difference	Strain gage transducer	172.4 kPa (25 psi)	±0.3 kPa (±0.05 psi)

[a]Label used in figure 2.

TABLE II. - FLOW TESTING OPERATING CONDITIONS
[Gas, pure nitrogen; gas temperature ≈ 0 °C]

Test pressure, MPa		
0.67	1.43	2.20
Nitrogen mass flow rate, g/s		
12.6	25.2	37.8
17.7	35.3	52.9
22.8	45.4	68.0
27.8	55.3	83.2
32.8	65.4	98.3
37.8	75.6	113.4

TABLE III. - P-40 STIRLING ENGINE DIMENSIONS
[NASA Lewis Research Center's P-40 Stirling engine was used for measurements]

Heater-tube manifolds	
Average hydraulic diameter, mm	5.0
Expansion space/heater-tube manifold average flow path length, mm	12.0
Heater tube/regenerator manifold average flow path length, mm	13.0
Cooler/compresssion-space connecting ducts	
Average hydraulic diameter, mm	14.0
Flow path length, mm	84.0
Cooler-tube manifolds	
Diameter, mm	48.0

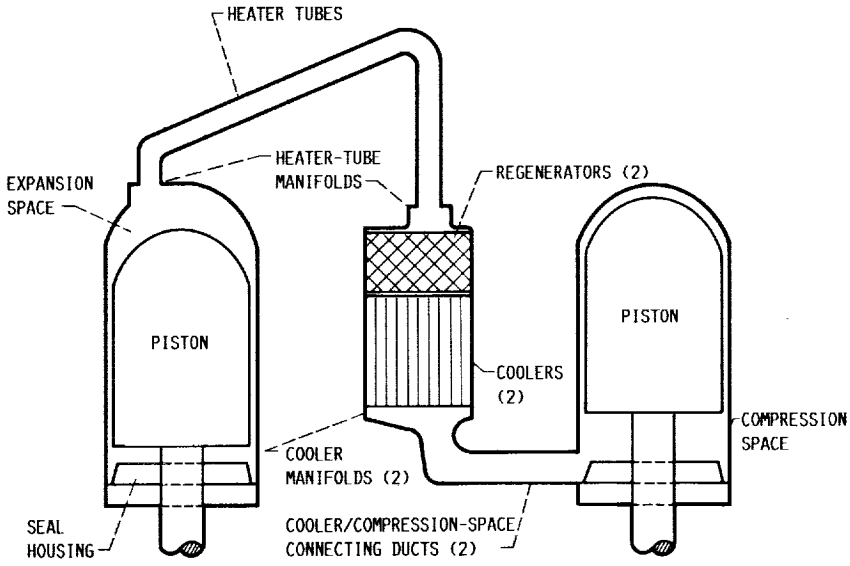

FIGURE 1. - DIAGRAM OF THE P-40 STIRLING ENGINE WORKING SPACE.

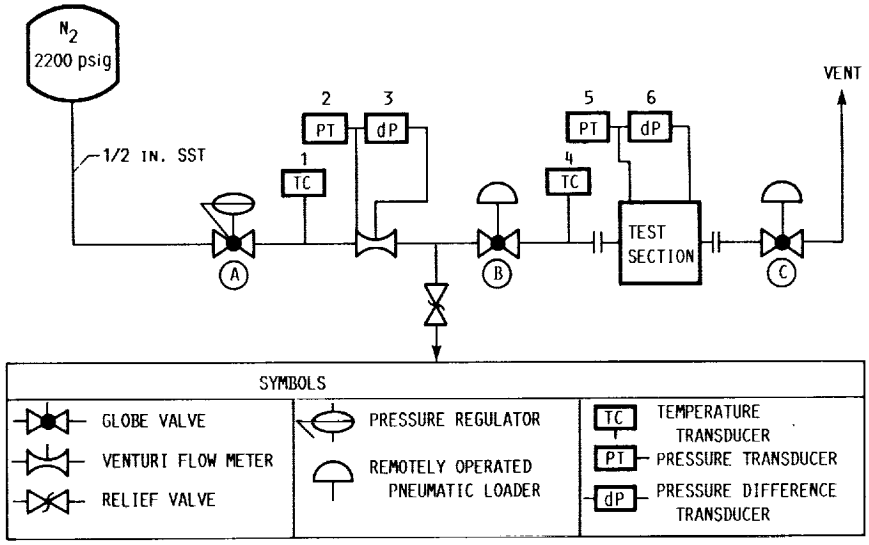

FIGURE 2. - FLOW TEST RIG SCHEMATIC.

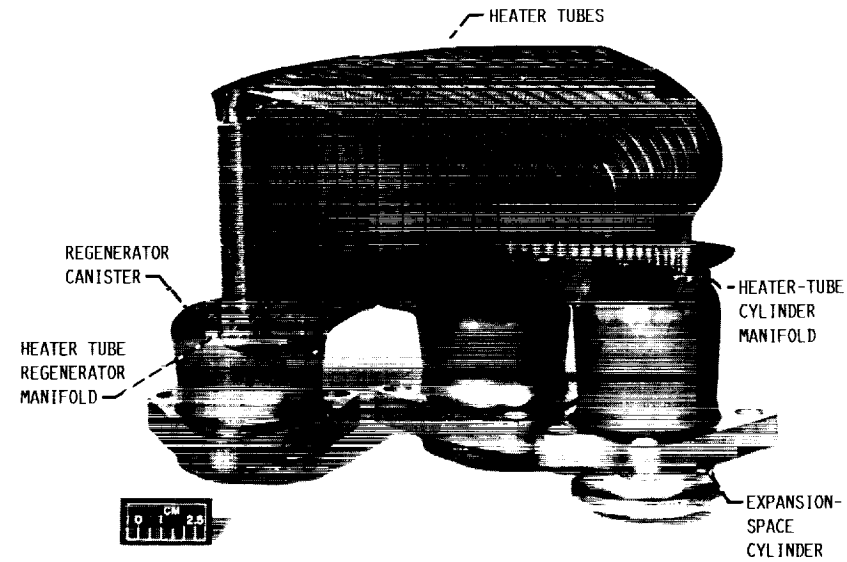

C-79-3984

(a) HEATER ASSEMBLY.

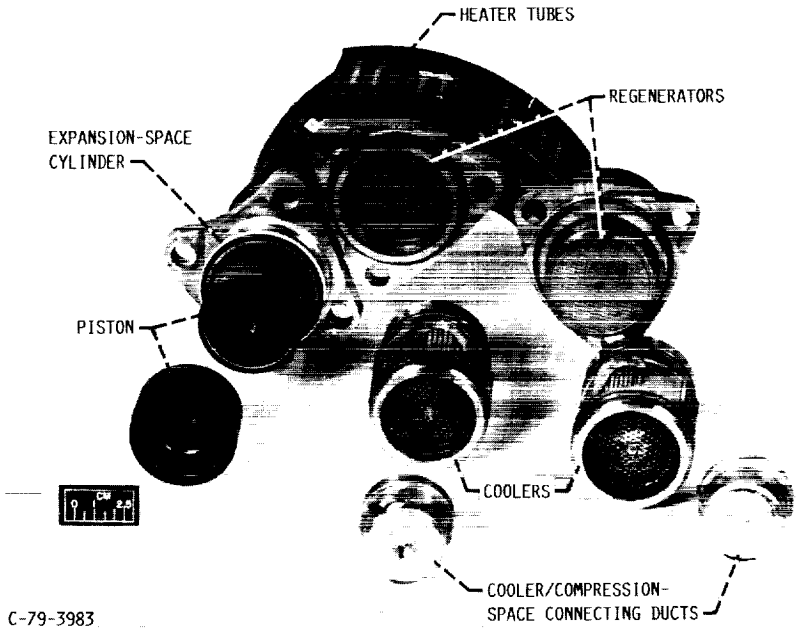

C-79-3983

(b) HEAT EXCHANGERS.

FIGURE 3. - P-40 STIRLING ENGINE HEAT EXCHANGERS AND HEATER ASSEMBLY.

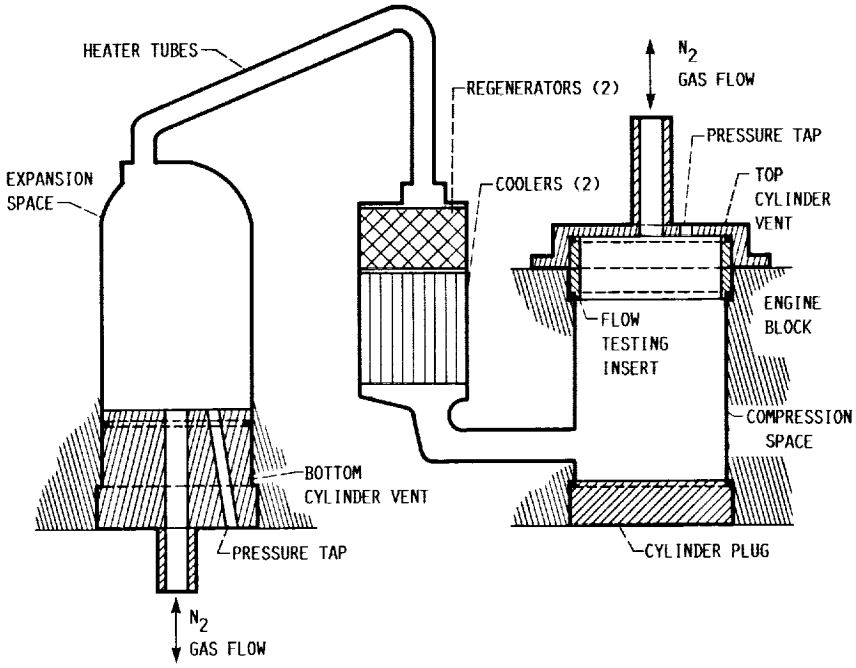

FIGURE 4. - DIAGRAM OF THE P-40 FLOW PATH TEST SECTION.

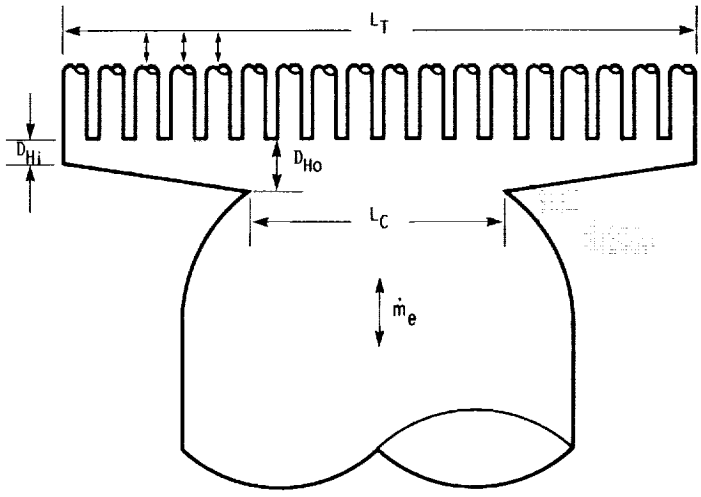

AVERAGE HYDRAULIC DIAMETER, $(D_{Hi} + D_{Ho})/2.0$

AVERAGE FLOW PATH LENGTH, $(L_T - L_C)/4.0$

EXIT MASS FLOW RATE, $\dot{m}_e$

FIGURE 5. - SIMPLIFIED DIAGRAM OF A HEATER TUBES MANIFOLD.

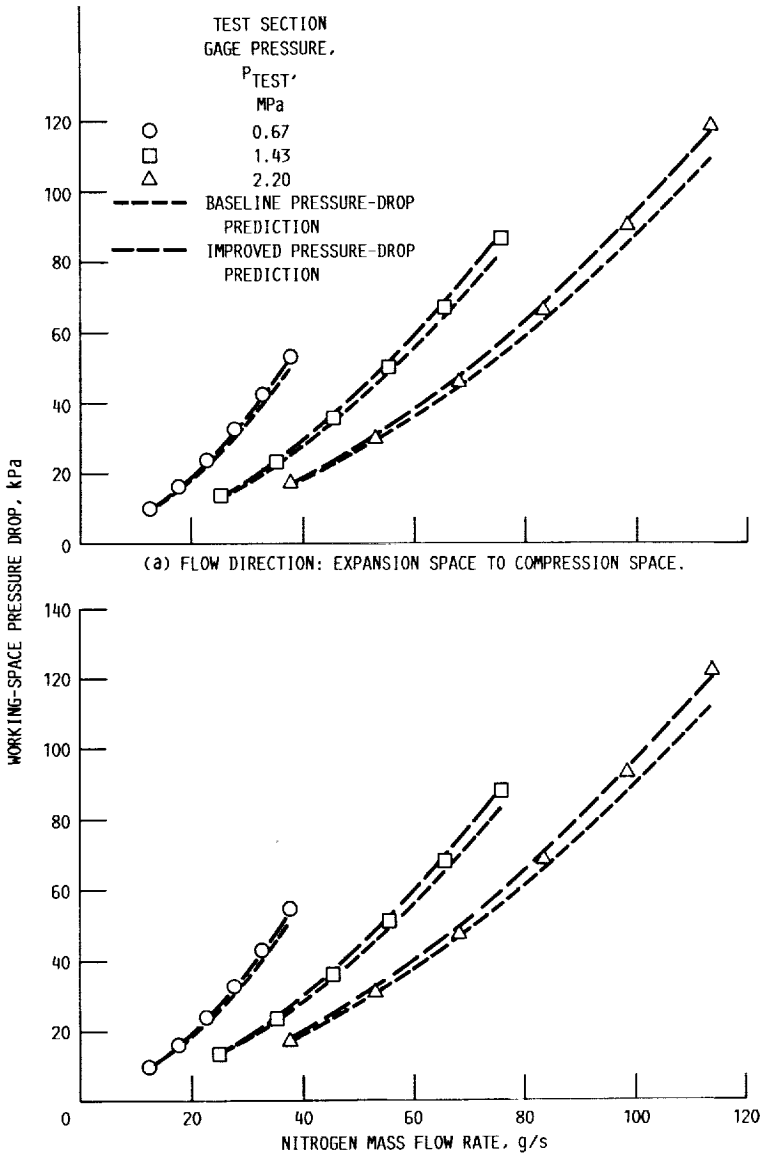

(a) FLOW DIRECTION: EXPANSION SPACE TO COMPRESSION SPACE.

(b) FLOW DIRECTION: COMPRESSION SPACE TO EXPANSION SPACE.

FIGURE 6. - FLOW TESTING DATA VERSUS PRESSURE-DROP PREDICTIONS DATA GATHERED FOR STEADY STATE CONDITIONS.

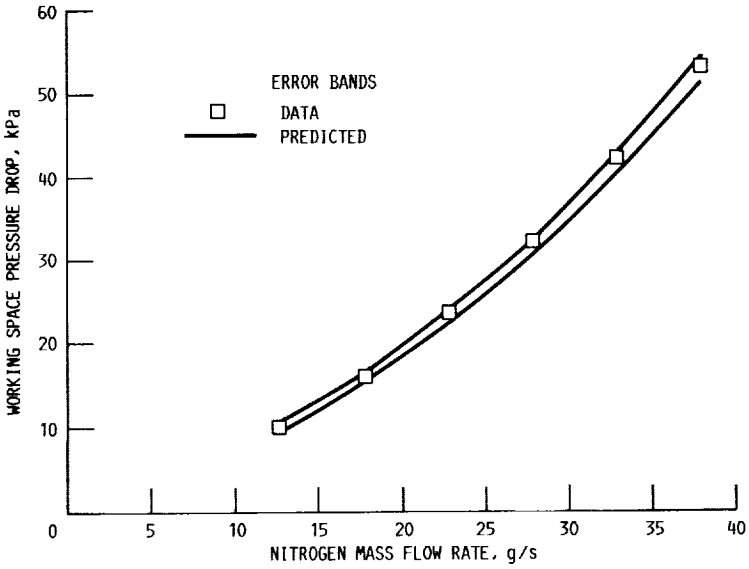

FIGURE 7. - PRESSURE DROP ERROR ANALYSIS RESULTS FOR FLOW TESTING DATA VERSUS IMPROVED PRESSURE-DROP PREDICTIONS. FLOW DIRECTION: EXPANSION SPACE TO COMPRESSION SPACE; TEST SECTION GAGE PRESSURE P_{TEST} = 0.67 MPa.

NASA
National Aeronautics and Space Administration

Report Documentation Page

1. Report No.	2. Government Accession No.	3. Reciplent's Catalog No.
NASA CR-182215 DOE/NASA/5266-1		

4. Title and Subtitle

Comparison of NASA Lewis Research Center's Performance Code's Pressure-Drop Model Predictions to Stirling Engine Working-Space Flow Test Data

5. Report Date: December 1988

6. Performing Organization Code:

7. Author(s)

Timothy J. Sullivan

8. Performing Organization Report No.: None

10. Work Unit No.: 778-35-13

9. Performing Organization Name and Address

Sverdrup Technology, Inc.
NASA Lewis Research Center Group
Cleveland, Ohio 44135-3191

11. Contract or Grant No.: NAS3-25266

13. Type of Report and Period Covered: Contractor Report, Final

12. Sponsoring Agency Name and Address

U.S. Department of Energy
Office of Vehicle and Engine R&D
Washington, D.C. 20545

14. Sponsoring Agency Code:

15. Supplementary Notes

Prepared under Interagency Agreement DE-AI01-85CE50112. Project Manager, Lanny G. Thieme, Power Technology Division, NASA Lewis Research Center, Cleveland, Ohio 44135.

16. Abstract

In support of the U.S. Department of Energy's Stirling Engine Highway Vehicle Systems program, the NASA Lewis Research Center's Stirling engine performance code's pressure-drop model was validated in this study. The validation was accomplished by comparing P-40 Stirling engine working-space pressure-drop prediction to experimental data for various steady flow test conditions. This report includes details of the flow test rig and the working-space pressure-drop predictions. After making various improvements to the Stirling engine pressure-drop model, the comparison showed good agreement between the working-space pressure drop predictions and the flow rig data.

17. Key Words (Suggested by Author(s))

Stirling engine
Code predictions
Flow test data

Date for general release December 1990.

Subject Category 44
DOE Category UC-96

19. Security Classif. (of this report)	20. Security Classif. (of this page)	21. No of pages	22. Price*
Unclassified	Unclassified	18	A03